



## TC-FLSFCL Provision for Improvement of Distribution System Reliability by TOPSIS based NSGA-II Method

Yashar Hashemi<sup>1</sup>, Khalil Valipour<sup>2</sup>

<sup>1,2</sup>Electrical Engineering Department, University of Mohaghegh Ardabili, Ardabil, Iran  
yashar\_hshm@yahoo.com, kh\_valipour@uma.ac.ir

### Abstract

An approach for assignment of the optimal location and tap changer adjustment related to flux-lock type superconducting fault current limiters with tap changer (TC-FLSFCL) is used in this paper by debating the reduction of fault current flowing from each device and enhancement of reliability varying with customer type in a distribution network connected with distribution generation (DG). TC-FLSFCL is a flexible SFCL that it has some preference than previous SFCLs. In this type of SFCL the current limiting characteristics are improved and the fault current limiting level during a fault period can be adjusted by controlling the current in third winding, which also made the magnetic field apply to the high-Tc superconducting (HTSC) element. Three objective functions based on reliability index, reduction of fault current and number of installed TC-FLSFCL is systematized and non-dominated sorting genetic algorithm-II (NSGA-II) style is then formed in searching for best location and tuning of tap changer of TC-FLSFCL to meet the fitness requirements. A decision-making procedure based on technique for order preference by similarity to ideal solution (TOPSIS) is used for finding best compromise solution from the set of Pareto-solutions obtained through NSGA-II. In a distribution network as Bus 4 of Roy Billinton test system (RBTS), comparative analysis of the results obtained from application of the resistive SFCL (RSFCL) and TC-FLSFCL is presented. The results show that optimal placement of TC-FLSFCL than RSFCL can improve reliability index and fault current reduction index with less number.

*Keywords:* NSGA-II, TC-FLSFCL, Reliability assessment, Distribution system, TOPSIS.

© 2013 IAUCTB-IJSEE Science. All rights reserved

### 1. Introduction

The electric power system has become more complicated and a fault current is getting larger due to the increasing electric power requirement. To increase reliability for power supply, the electric power systems are interconnected each other to give and take the electric power. The interconnection of power system is restricted to a certain extent so that the fault current will not exceed a circuit breaker (C.B) capacity and the fault point can be rejected from the power system by the C.B. not expand the influence of the fault when it occurs. Also in recent years, power generation companies have tented to the use of distribution generation resources due to

several reasons, like deregulation, restructuring, advances in technology, environmental policies and increased demand for the electricity. Along with its benefits, distribution generation may have negative impacts on the distribution system since it increase the fault current level and changes the direction of the flow of current in the lines during fault situation. The most important negative consequences can be mentioned as false tripping and/or reduction of reach of protective device and missing the coordination between such devices.

The most common methods to reduce high-level fault currents and their disadvantages can be expressed as below:

- a) Substitution and upgrading of components: this solution is a relatively expensive solution if transformers and cables or overhead lines are also involved.
- b) Sequential switching: this procedure has some safety risks to people and equipments if it fails to prevent the circuit breaker opening before the fault current has been reduced sufficiently.
- c) Using a power electronic converter interface for distribution generations (DGs). Unfortunately, this method suffers from higher power rating, weight and cost if it be used as fault current limiter.
- d) Active fault level management: this solution is an early stage of development and will be very expensive at least in near future.
- e) Network splitting and reconfiguration that suffers from reducing the power quality of network due to the increased source impedance and system losses.
- f) Increasing impedance (e.g. by current limiting reactor (CLR) or high-impedance transformers) that needs additional effort to maintain the voltage profile, and increases the network losses.

Fault current limiters (FCLs) are expected to improve reliability and stability of power systems by reducing the fault current [1]. Many studies on FCLs have been carried out [2]. Up to now, several kinds of SFCL have been proposed and it is expected that they will be applied to appropriate position considering their own properties [3] and [4]. Amongst those proposed SFCL, the flux-lock type SFCL (FLSFCL) has some advantages; the current limiting characteristics are improved, and the amplitude of initial fault current can be adjusted [5]. A type SFCL which consists of a flux-lock reactor with a high-Tc superconducting (HTSC) element and magnetic field winding can increase both the initial limiting current level and limiting impedance simultaneously by a transformer action and magnetic field application. In FLSFCL proposed in [6] the number of turns of third winding can be adjusted with a tap changer. In this type of SFCL line current is affected by the current in third winding, which can be adjusted through a tap changer.

From a viewpoint of power system planning, it is desired to develop a method to find suitable locations of SFCL in power system. When an SFCL is introduced in an electric power grid (EPG), two important factors must be considered: a) optimal location of the SFCL in the EPG, b) optimal impedance value of the SFCL. Various procedures have been expanded for defining the optimal location assignment of SFCLs in an electric power system. Criteria that is used in numerous cases for specifying the optimal location of SFCLs consist of the total SFCL capacity [7], sensitivity [8], and fault current

reduction [9]. References [7] and [10] describe how genetic algorithm can be used to find the optimal placements of the minimum number of FCLs to meet maximum fault current objectives. After specifying a maximum desired fault current, combinations of FCLs at different locations are compared to find the optimal placements. The impedances and number of devices are regarded as a weight to optimize grouping. With this method, the minimum number and minimum impedances of FCLs were applied to satisfy the limitation of fault currents. For the case of an original system with newly added DG, references [11] and [12] analysed the influence on the relay scheme of FCLs, which are installed in several possible locations in the original system. The study proved that when the FCL is located near the DG, it limits the fault current while minimizing the problem associated with the protection scheme. These papers reveal the best placements in the utility grids. In [13] an approach to select optimal location of a RSFCL in an EPG has been presented. This work is based on the study of the angular separation between the rotors of the generators present in the power system. FCL technology competes with the old-fashioned breaker upgrading solution as alternatives available for the fault current over duty problem in existing substations. As a matter of fact, reliability and economics are two conflicting aspects to be analyzed for the ultimate decision making, thus reference [14] assess reliability of substation architectures accommodating the FCL operation and besides, numerically surveys the FCL effects on the substation reliability indices.

The main contribution of this paper is optimal site assignment and tap changer adopting of TC-FLSFCL according to reduction of fault current and amelioration of reliability in a distribution network connected to distributed generation. TC-FLSFCL as pliable SFCL has advantages related to: a) changeable inductance of third winding; that it possible to the fault current limiting level during a fault period be adjusted by controlling the current in third winding, which made the magnetic field apply to the HTSC element. b) Ameliorating the current limiting characteristics. Multi-objective optimization for placement and designing of a TC-FLSFCL is performed. Used fitness functions are the decrement of fault current and reliability index. With regard to privilege of NSGA-II optimization method, this style is utilized to solve the problem. Multi-attribute decision-making (MADM) approach based on TOPSIS method is adopted to rank the Pareto-optimal solutions from the best to the worst and to determine the best solution in a deterministic environment with a single decision maker. With case study applied to a distribution network a comparative

analysis between the results from application of the TC-FLSFCL and RSFCL is presented.

## 2. Flux-lock-type SFCL with a tap-changer

Fig. 1 shows a fundamental configuration of a flux-lock type SFCL (FLSFCL) with a high  $T_c$  superconducting. The FLSFCL consists of a flux-lock reactor and magnetic field winding circuit. The former is composed of winding 1 and winding 2 which are connected in parallel with each other through an HTSC element. The latter is constructed by winding 3, a magnetic field winding, a series resistor and phase adjusting capacitor. Windings 1, 2 and 3 are densely wound on the same core to reduce the leakage flux. The two winding of the flux-lock reactor are wound to counteract each other flux. The voltage across the windings 1, 2, 3 are given by:

$$v_1 = n_1 \frac{d\Phi_1}{dt}, v_2 = -n_2 \frac{d\Phi_3}{dt}, v_3 = n_3 \frac{d\Phi_3}{dt} \quad (1)$$

Where,  $n_1, n_2, n_3$  are numbers of turns of the windings and  $\Phi$  is the magnetic flux through the iron core i.e. the flux linkage commonly in the three windings. Under normal status when load current passes through the SFCL, the HTSC element is in superconducting state, so that the voltage across the element is zero. Then winding 1 and 2 are directly connected in parallel, thus:

$$v_1 = v_2 \quad (2)$$

From (1), we get:

$$(n_1 + n_2) \frac{d\Phi}{dt} = 0 \quad (3)$$

Since  $n_1 + n_2 \neq 0$ , it follows that

$$\frac{d\Phi}{dt} = 0 \quad (4)$$

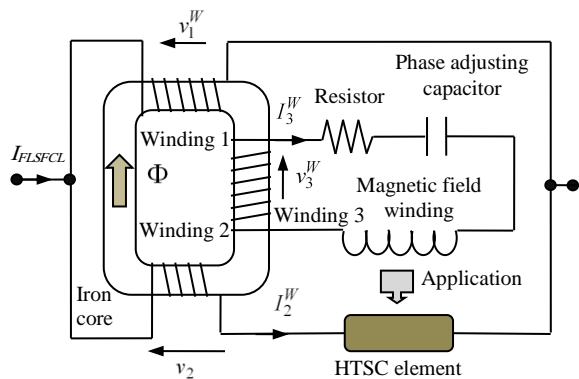


Fig.1. Fundamental configuration of the FLSFCL

Equation (4) implies that the linkage flux is locked in a DC mode, so that the voltage across the three windings must be zero. In other word, negligible low impedance is realized in the SFCL for a normal load current. Furthermore, the field current  $i_f$  does not flow in this case, and the HTSC element is

not exposed to magnetic field. Thus, no deterioration of the critical current by external magnetic field is brought about in a superconducting state of the HTSC element. When the HTSC element loses its superconducting and has somewhat resistance due to an overcurrent, (2) and (3) are no longer established. Thus  $\Phi$  varies with time and the voltage across the windings are induced. In consequence, impedance appears in the FCL, so that the overcurrent can be reduced. Simultaneously,  $i_f$  flows in the magnetic field winding and then the external AC magnetic field is applied to the HTSC element. This operation causes the resistance of the element to get higher effectively. This FCL has a self-triggering mechanism and no addition external power source for applying magnetic field.

In order to adjust the current for generation of the magnetic field applied to HTSC element, the FLSFCL with a tap-changer in third winding is used [6] that it has the same operational principle as the FLSFCL. Because the HTSC element has no resistance, the magnetic flux induced by winding 1 and 2 in normal status is eliminated. So, no magnetic field from the magnet field winding is not applied to the HTSC element. The resistance of the HTSC element under fault status reveals. It leads the magnetic flux by windings 1 and 2 to link the winding 3, in which the magnetic field can be applied to the HTSC element and the resistance of HTSC element increases. The adjustment action is conducted by a tap-changer. For analysis of the circuit equivalent for the TC-FLSFCL, the Fig. 2 can be considered.

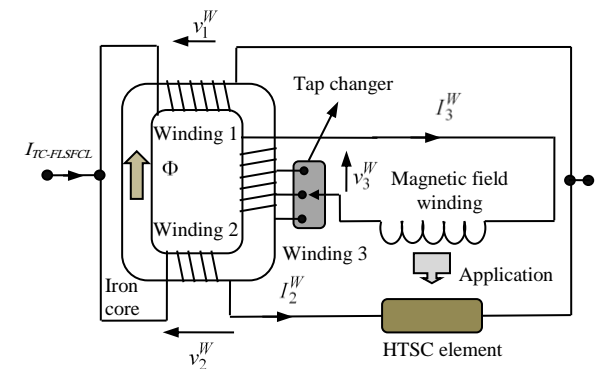


Fig.2. Fundamental configuration of the TC-FLSFCL.

Finite-differential method (FDM) for circuit analysis of the equivalent circuit for the TC-FLSFCL is used as shown in Fig. 3.

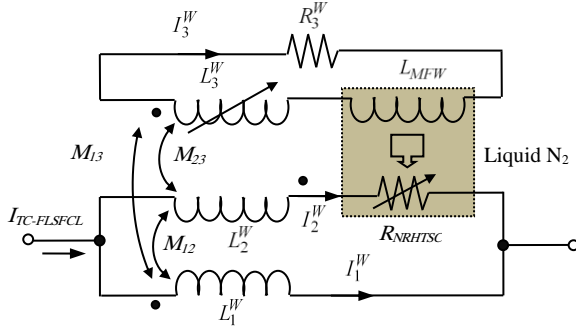


Fig. 3. Equivalent circuit of the TC-FLSFCL.

In this figure  $R_{NRHTSC}$  and  $L_{MFW}$  are the normal resistance of HTSC element and the inductance of magnetic field winding. Assuming that coupling coefficients between two windings were one and that the leakage flux and resistance of windings 1, 2 and 3 are negligible, the fault impedance ( $Z_{TC-FLSFCL}$ ) and currents ( $I_1^W$ ,  $I_{TC-FLSFCL}$ ,  $I_3^W$  as shown in Fig. 3) in windings 1, 2 and 3, which is expressed by the ratio for line current ( $I_{TC-FLSFCL}$ ), can be deduced as following equations [6]:

$$Z_{TC-FLSFCL} = \frac{R_{NRHTSC} L_1^W (-\omega^2 L_{MFW} + j\omega R_{MFW})}{R_{MFW} R_{NRHTSC} - \omega^2 L_{MFW} L^2 + j\omega(L^2 R_{MFW} + L_{MFW} R_{NRHTSC} + L_3^W R_{NRHTSC})} \quad (5)$$

$$\frac{I_1^W}{I_{TC-FLSFCL}} = \frac{R_{NRHTSC} R_{MFW} - \omega^2 L_{MFW} L(L - \sqrt{L_1^W})}{R_{MFW} R_{NRHTSC} - \omega^2 L_{MFW} L^2 + j\omega(L^2 R_{MFW} + L_{MFW} R_{NRHTSC} + L_3^W R_{NRHTSC})} + \frac{j\omega [L R_{MFW} (L - \sqrt{L_1^W}) + R_{NRHTSC} (L_{MFW} + L_3^W)]}{R_{MFW} R_{NRHTSC} - \omega^2 L_{MFW} L^2 + j\omega(L^2 R_{MFW} + L_{MFW} R_{NRHTSC} + L_3^W R_{NRHTSC})} \quad (6)$$

$$\frac{I_2^W}{I_{TC-FLSFCL}} = \frac{(-\omega^2 \sqrt{L_1^W} L_{MFW} L + j\omega \sqrt{L_1^W} L R_{MFW})}{R_{MFW} R_{NRHTSC} - \omega^2 L_{MFW} L^2 + j\omega(L^2 R_{MFW} + L_{MFW} R_{NRHTSC} + L_3^W R_{NRHTSC})} \quad (7)$$

$$\frac{I_3^W}{I_{TC-FLSFCL}} = \frac{j\omega \sqrt{L_3^W} L_3^W \cdot R_{NRHTSC}}{R_{MFW} R_{NRHTSC} - \omega^2 L_{MFW} L^2 + j\omega(L^2 R_{MFW} + L_{MFW} R_{NRHTSC} + L_3^W R_{NRHTSC})} \quad (8)$$

where  $L = \sqrt{L_1^W} \pm \sqrt{L_2^W}$ .

### 3. Formulation of the problem

The addition of DGs to a power system can increase the fault current levels and thereby affect the relay coordination. The increase in the maximum fault current due to the presence of new DGs may make new protective devices with higher breaking capacities necessary. In addition, modification of the relay coordination may also be required, since the changes in the fault current patterns caused by the DGs can affect the relay coordination. The strategic placement of SFCLs can help reduce the maximum fault current to within the breaking capacity of the protective devices. In this study, the multi-criteria SFCL placement problem is surveyed [15].

The index of fault current reduction is defined as  $j^{\text{th}}$  devices fault current deviation in a network with SFCL and without. Simultaneously, this deviation is applied to weighting factor  $\omega_j$  for  $j^{\text{th}}$  device among the total number of devices  $N_D$ , which

is calculated by the devices cost. The objective function related to the reduction in average fault current due to the installation of SFCL can be expressed as follows:

$$FCRI = \sum_{j=1}^{N_D} \omega_j (I_j^{\text{Without SFCL}} - I_j^{\text{With SFCL}}) \quad (9)$$

When a new device is connected in series to a system, the reliability of the system commonly deteriorates. The SFCL, in contrast, not only decrease the stresses on most of the devices in a network but also reduces the frequency of the excessive fault current, thereby often improving the failure rate of devices. Therefore, the changes of reliability for existing devices should be estimated in order to evaluate the reliability of distribution networks connected with the SFCL as a new device. The magnitude of fault currents flowing in a

protective device depends on a location where a fault occurs. If the SFCL is installed in a network, fault currents will be reduced due to the inherent characteristic of the SFCL to limit fault currents in a network. There are various reasons causing the fault in a protective device such as degraded operation, worn, arcing, and fault current. It is assumed that these reasons are independent of each other, and then, the failure rate of the  $j$ th protective device is given as:

$$\begin{aligned} \lambda_j^{Without SFCL} = & \lambda_j^{Without SFCL, fault current} + \\ & \lambda_{0,j}^{Without SFCL, degraded operation} + \\ & \lambda_j^{Without SFCL, worn} + \lambda_j^{Without SFCL, arcing} + \dots \end{aligned} \quad (10)$$

As a result, the failure rate of the  $k$ th protective device after the installation of SFCL is determined as follows:

$$\lambda_{k,f}^{With SFCL} = \lambda_{k,f}^{Without SFCL} - \lambda_{k,f}^{Without SFCL, fault current} \eta_{k,f}^{With SFCL} \quad (11)$$

Where,  $\lambda_j^{Without SFCL, fault current}$  is the failure rate only caused by fault current for failure event  $f$  at  $k^{\text{th}}$  load when SFCL does not exist in a network  $\eta_{k,f}^{With SFCL}$  is the fault current reduction efficiency of failure event  $f$  at  $k^{\text{th}}$  load when SFCL is installed.

In order to estimate distribution reliability, weighted-load reliability index (WLRI) is used and its details is described briefly as follows [15]:

$$\begin{aligned} WLRI_k^{With SFCL} = & \sum_{m=1}^3 \omega_m R^{With SFCL}(m,k) \\ R^{With SFCL}(m,k) = & \begin{cases} \frac{\sum_{f \in \Lambda \text{ failur events}} \lambda_{k,f}^{With SFCL} N_k}{\sum_{k=1}^K N_k} & (m=1) \\ \frac{\sum_{f \in \Lambda \text{ failur events}} r_{k,f}^{With SFCL} N_k}{8760 \sum_{k=1}^K N_k} & (m=2) \\ \frac{\sum_{f \in \Lambda \text{ failur events}} r_{k,f}^{With SFCL} P_k}{\sum_{k=1}^K N_k} & (m=3) \end{cases} \end{aligned} \quad (12)$$

Where,  $\omega_m$  is the normalization factor for the value of  $m^{\text{th}}$  reliability, and  $r_{k,f}^{With SFCL}$ ,  $N_k$ ,  $P_k$  are repair time, the number of customers and the amount of electric demand power, respectively. A criterion to measure the reliability improvement by the change of distribution reliability according to an installation

location of SFCL is reliability sensitivity index that can be characterized as follows:

$$\begin{aligned} RSI^{With SFCL} = & \sum_{k=1}^K \omega_k (WLRI_k^{Without SFCL} - WLRI_k^{With SFCL}) \quad (13) \\ \omega_k = & \frac{CIC \text{ of } k\text{th load point}}{\text{average CIC all types of customers}} \end{aligned}$$

Where,  $RSI^{With SFCL}$  represents RS when SFCL is installed in network, and  $\omega_k (WLRI_k^{Without SFCL} - WLRI_k^{With SFCL})$  is the amount of weighted-load reliability deviation for  $k^{\text{th}}$  load before SFCL is installed and after.  $\omega_k$  is determined by considering customer interruption cost (CIC) of each customer as a weighting factor by the significance of  $k^{\text{th}}$  load.

In addition to the fault current reduction index and reliability sensitivity index, the number of SFCLs is also considered in finding the optimal placement of SFCLs. The objective function related to the number of SFCLs, can be expressed as follows:

$$\begin{aligned} \text{Minimize } N_{SFCL} \quad (14) \\ N_{SFCL} \text{ is the Number of SFCLs to be installed.} \end{aligned}$$

Mathematically, (9)-(14) can be proposed as following optimization problem:

$$\begin{aligned} \text{Min} \{ -FCRI, -RSI, N_{SFCL} \} = \\ \text{Min} \left\{ \sum_{j=1}^{N_D} \omega_j (I_j^{Without SFCL} - I_j^{With SFCL}), \right. \\ \left. \sum_{k=1}^K \omega_k (WLRI_k^{Without SFCL} - WLRI_k^{With SFCL}), N_{SFCL} \right\} \quad (15) \end{aligned}$$

#### 4. NSGA-II implementation to optimal placement and design of TC-FLSFCL

The NSGA-II algorithm and its detailed implementation procedure can be found in [16] and [17]. This algorithm has been demonstrated to be among the most efficient algorithms for multi-objective optimization on a number of benchmark problems. NSGA-II uses non-dominated sorting for objective assignments. Front number 1 are assigned as all individuals not dominated by any other individuals. All individuals only dominated by individuals in front number 1 are assigned front number 2, and so on. Selection proceeding is conducted, using tournament between two individuals. If the two individuals are from different fronts the individual with the lowest front number is

selected. The individual with the highest crowding distance is selected if they are from the same front, i.e., a higher fitness is assigned to individuals located on a sparsely populated part of the front. In every iteration,  $N$  new individuals (offspring) are generated. The parents also have  $N$  individuals. Both these parents and offspring compete with each other for inclusion in the next iteration.

**Simulated Binary Crossover (SBX):** The simulated binary crossover operator works with two parent solutions and creates two offspring. The crossover index " $\eta_c$ " is any nonnegative real number. A large value of " $\eta_c$ " gives a higher probability for creating "near-parent" solutions and a small value of " $\eta_c$ " allows distant solutions to be selected as offspring. The two offspring created are symmetric about the parent solutions. Also, for a fixed " $\eta_c$ ", the offspring have a spread which is proportional to that of the parent solutions. Essentially, the simulated binary crossover operator has two properties:

- The distinction between the offspring is in proportion to the parent solution.
- Near-parent solutions become mostly offspring than solutions distant from parents.

**Polynomial Mutation:** The probability distribution is a polynomial function. The probability of creating a solution closer to the parent is more than the probability of creating one away from it. The form of the probability distribution is directly controlled by an external parameter " $\eta_m$ ", and the distribution is not dynamically changed with iterations.

## 5. TOPSIS method

When solutions based on the estimated Pareto-optimal set are found, it is required to choose one of them for implementation. From a decision maker's perspective, the choice of a solution from all Pareto-optimal solutions is called a posteriori approach and it requires high-level decision-making approach which is to determine the best solution among a finite set of Pareto-optimal solutions with respect to all relevant attributes. MADM techniques are generally employed in posterior evaluation of Pareto-optimal solutions to choose the best one among them. The decision making problem for alternatives selection usually called multiple attribute decision making, which has been proven to be an effective approach for ranking or selecting one alternative from a finite set of alternatives with respect to multiple, usually conflicting attributes. The selected alternative has the highest degree of satisfaction for all of the relevant attributes, and term "attribute" is referred to as a goal or criterion. A large number of methods have been developed for selecting best compromise solution in

multiple attribute or multiple criteria problems. The concept of TOPSIS is used for finding best compromise solution in this paper. TOPSIS method was developed from the concept that the selected feasible scheme should be close to the ideal solution but far to the negative ideal solution [18], and it has become a common method in multi-objective decision-making from finite alternatives [19]. Assuming that  $R = \{R_{ij} | i = 1, 2, \dots, n; j = 1, 2, \dots, m\}$

( $n, m$  are the number of Pareto-optimal solutions and number of objectives respectively) be the  $n \times m$  decision matrix, where  $R_{ij}$  is the performance rating of alternative  $X_j$  (Pareto-optimal solution) with respect to attribute  $A_i$  (objective function values). To determine objective weights by the entropy measure, the decision matrix needs to be normalized for each objective  $A_j$  as:

$$p_{ij} = \frac{R_{ij}}{\sum_{p=1}^n R_{pj}} \quad (16)$$

As a consequence, a normalized decision matrix representing the relative performance of the alternatives is obtained as

$$P = \begin{bmatrix} p_{11} & p_{12} & \dots & p_{1m} \\ p_{21} & p_{22} & \dots & p_{2m} \\ \dots & \dots & \dots & \dots \\ p_{n1} & p_{n2} & \dots & p_{nm} \end{bmatrix} \quad (17)$$

The amount of decision information contained in (17) and emitted from attribute  $A_j$  ( $j=1, 2, \dots, m$ ) can thus be measured by the entropy value as:

$$e_j = \frac{-1}{\ln n} \sum_{i=1}^n p_{ij} \ln(p_{ij}) \quad (18)$$

The degree of divergence ( $d_j$ ) of the average intrinsic information contained by each attribute  $A_j$  ( $j=1, 2, \dots, m$ ) can be calculated as:

$$d_j = 1 - e_j \quad (19)$$

The objective weighted normalized value  $v_{ij}$  is calculated as

$$v_{ij} = w_i p_{ij} \quad (20)$$

After determining performance ratings of the alternatives and objective weights of attributes, the next step is to aggregate them to produce an overall performance index for each alternative. This aggregation process is based on the positive ideal solution ( $A^+$ ) and the negative ideal solution ( $A^-$ ), which are defined, respectively, by:

$$\begin{aligned} A^+ &= (\max(v_{i1}) \quad \max(v_{i2}) \quad \dots \quad \max(v_{im})) = (v_1^+, v_2^+, \dots, v_m^+) \\ A^- &= (\min(v_{i1}) \quad \min(v_{i2}) \quad \dots \quad \min(v_{im})) = (v_1^-, v_2^-, \dots, v_m^-) \end{aligned} \quad (21)$$

Separation (distance) between alternatives can be measured by the  $n$ -dimensional Euclidean distance. The separation of each alternative from the ideal solution is given as:

$$d_j^+ = \left\{ \sum_{i=1}^m (v_{ji} - v_i^+)^2 \right\}^{1/2}, \quad j = 1, 2, \dots, n \quad (22)$$

Similarly, the separation from the negative ideal solution is given as:

$$d_j^- = \left\{ \sum_{i=1}^m (v_{ji} - v_i^-)^2 \right\}^{1/2}, \quad j = 1, 2, \dots, n \quad (23)$$

The relative closeness to the ideal solution of alternative  $X_j$  with respect to  $A^+$  is defined as:

$$C_j = \frac{d_j^-}{d_j^+ + d_j^-}, \quad j = 1, 2, \dots, n \quad (24)$$

Since  $d_j^- \geq 0$  and  $d_j^+ \geq 0$ , then, clearly,  $C_j \in [0, 1]$ .

Choose an alternative with maximum  $C_j$ , in descending order. It is clear that an alternatives  $X_j$  is closer to  $A^+$  than to  $A^-$  as  $C_j$  approaches 1.

## 6. Case Study and Results

In this study, Bus 4 of the RBTS is used to evaluate the design and placement of TC-FLSFCL where two DG is connected with network as output data given in Table 1. The RBTS has been used as a reference for many reliability studies and evaluation techniques in the literature. A description of the RBTS and its system data can be found in [20] and [21]. The advantage of the RBTS is the availability of the practical reliability data for all components. The single line diagram for the study system is shown in Fig. 4.

Failure rates of circuit breaker, line switch and 138/33 KV transformer only caused by fault current are 0.0015, 0.0017 and 0.0047 respectively. A balanced three-phase short circuit is simulated to entire lines in network. Fault current for each device is analyzed. Then the device failure rate can be estimated. Weighting factors of the circuit breaker, line switch and fuse are 2.3, 0.319 and 0.0017 respectively. The weighting factors by CIC of customers are postulated based on the data in [22]. Customer, device reliability, system data and parameters of TC-FLSFCL are given in Tables 2, 3

and 4. The placement and tuning of TC-FLSFCL is handled as multi-objective optimization problem where index of fault current reduction, reliability sensitivity index and number of SFCL are optimized simultaneously with NSGA-II algorithm. The flowchart of the proposed method is shown in Fig. 5. The Pareto-optimal set with NSGA-II in two-dimensional and three-dimensional objective function for TC-FLSFCL and RSFCL is represented in Figs. 6 and 7. A decision making procedure based on TOPSIS method is conducted to find the best compromise solution from the set of Pareto-solutions obtained using NSGA-II. Table 5 shows the best compromise solution obtained using TOPSIS method for NSGA-II.

The optimal number of SFCL, fault current reduction index and reliability sensitivity index in two different cases as: case 1) RSFCL and case 2) TC-FLSFCL are shown in Table 6. TOPSIS based NSGA-II is used to solve the proposed optimization problem which is a nonlinear mixed integer optimization problem and its performance is compared with TOPSIS based ordinary MOPSO. Comparison of different options shows that in the state that we use TC-FLSFCL, two TC-FLSFCL are needed. In contrast, the optimal number of RSFCL is four. This is due to optimal tuning of tap changer for controlling the current in winding 3. As indicated in Table 6 and Fig. 8 the fault current reduction index is highest when TC-FLSFCL is applied where optimal number of TC-FLSFCL is lower than the optimal number of RSFCL. Also, the TOPSIS based NSGA-II results in a better performance.

## 7. Conclusions and discussions

Implementation of TC-FLSFCL for reduction of fault current and improvement of the power system reliability is proposed. Flexibility, improved current limiting characteristics and adjustable fault current limiting level during a fault period incentive to use TC-FLSFCL for amelioration of reliability system and fault current reduction. TC-FLSFCL is a type of FLSFCL that can increase the resistance of the HTSC element by AC magnetic field winding, which is constructed in third winding. The current flowing at the third winding, which is connected with magnetic field winding, affects the fault current limiting characteristics. In this type of FLSFCL the current for generation of magnetic field applied to HTSC element can be adjusted by changing inductance of third winding through a tap changer. Thus by controlling the current in third winding which also made the magnetic field apply to the HTSC element, the fault current limiting level during a fault period can be adjusted. A three objective optimization approach organized of fault current reduction, reliability index and number of installed

TC-FLSFCL is systematized and NSGA-II method is then utilized for best location and modulating of tap changer of TC-FLSFCL to reach the fitness requirement. From a decision maker perspective, an approach based on TOPSIS method is used to determine solutions with respect to all relevant attributes from the set of Pareto-solutions obtained

using NSGA-II. A comparative performance study of a RSFCL and TC-FLSFCL has been carried out on modified distribution system of RBTS bus 4. The results obtained from test case demonstrate that optimal placement and tuning of TC-FLSFCL than RSFCL can enhance the power system reliability and fault current reduction criterion.

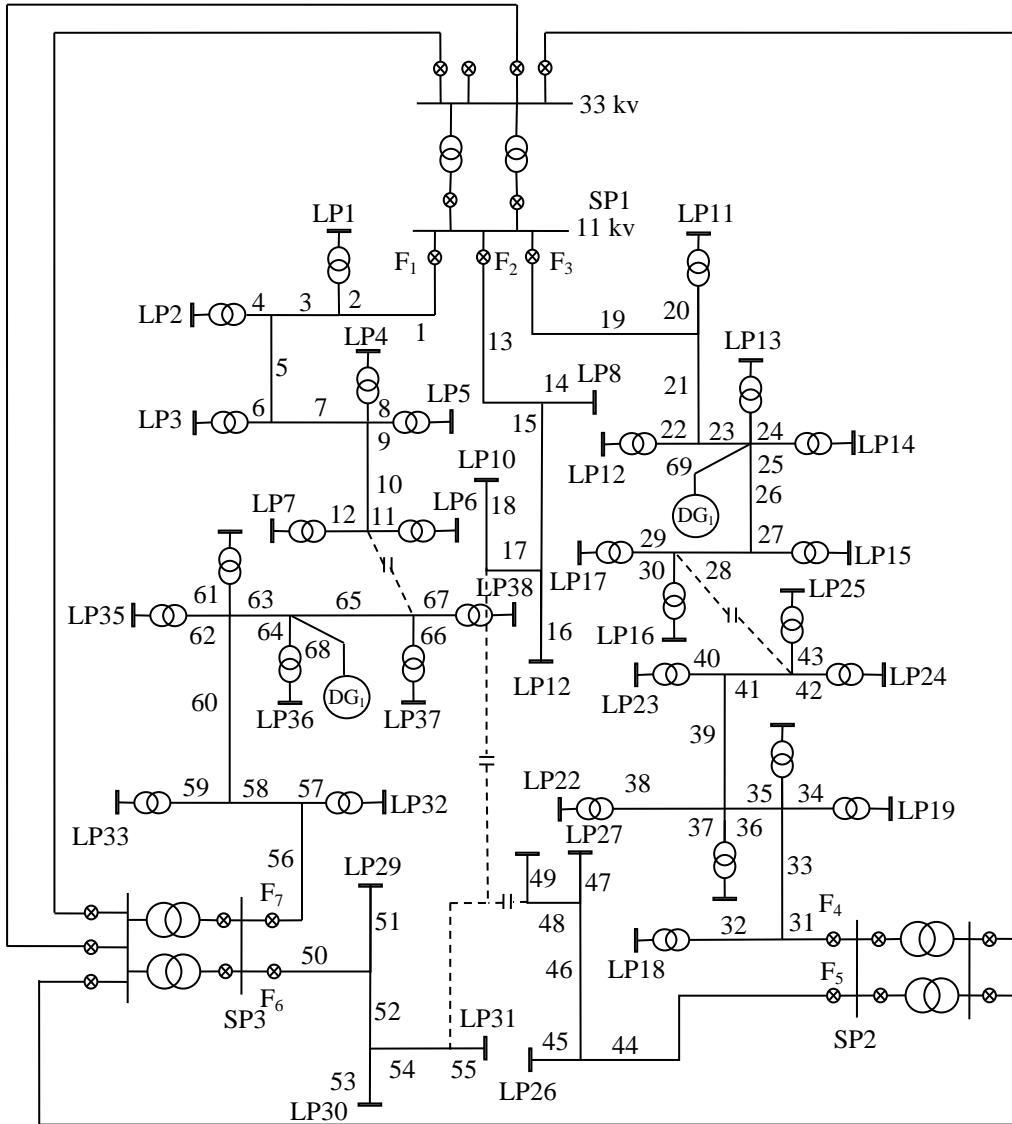


Fig.4: Distribution system for RBTS bus 4

Table.1  
The output of DG

	Generation	
	MW	MVAR
DG <sub>1</sub>	1.7	0.6
DG <sub>2</sub>	1.5	0.7

Table.2  
Customer data

k	Load points	Customer type	Load level per load point (MW)		Number of customers	$W_k$
			Average	Peak		
1	LP1	residential	0.545	0.8869	220	0.6
2	LP2	residential	0.545	0.8869	220	0.6
3	LP3	residential	0.545	0.8869	220	0.6
4	LP4	residential	0.545	0.8869	220	0.6
5	LP5	residential	0.500	0.8137	200	0.6
6	LP6	commercial	0.415	0.6714	10	1.8
7	LP7	commercial	0.415	0.6714	10	1.3
8	LP8	small user	1.00	1.63	1	1.4
9	LP9	small user	1.50	2.445	1	0.3
10	LP10	small user	1.00	1.63	1	0.3
11	LP11	residential	0.545	0.8869	220	0.5
12	LP12	residential	0.545	0.8869	220	0.5
13	LP13	residential	0.545	0.8869	220	0.5
14	LP14	residential	0.500	0.8137	200	0.5
15	LP15	residential	0.500	0.8137	200	0.5
16	LP16	commercial	0.415	0.6714	10	1.9
17	LP17	commercial	0.415	0.6714	10	1.5
18	LP18	residential	0.545	0.8869	220	0.7
19	LP19	residential	0.545	0.8869	220	0.7
20	LP20	residential	0.545	0.8869	220	0.7
21	LP21	residential	0.545	0.8869	220	0.7
22	LP22	residential	0.500	0.8137	200	0.7
23	LP23	residential	0.500	0.8137	200	0.7
24	LP24	commercial	0.415	0.6714	10	1.6
25	LP25	commercial	0.415	0.6714	10	1.6
26	LP26	small user	1.00	1.63	1	0.4
27	LP27	small user	1.00	1.63	1	0.4
28	LP28	small user	1.00	1.63	1	0.4
29	LP29	small user	1.00	1.63	1	0.4
30	LP30	small user	1.00	1.63	1	0.4
31	LP31	small user	1.50	2.445	1	0.4
32	LP32	residential	0.545	0.8869	220	0.4
33	LP33	residential	0.545	0.8869	220	0.4
34	LP34	residential	0.545	0.8869	220	0.4
35	LP35	residential	0.545	0.8869	220	0.4
36	LP36	residential	0.500	0.8137	200	0.4
37	LP37	residential	0.500	0.8137	200	0.4
38	LP38	commercial	0.415	0.6714	10	1.7

Table.3  
Reliability and system data

Component	Failure rate (f/yr) [for lines/cables (f/yr.km)]	Repair time (hr)
transformers		
33/11 kV	0.0150	15
breakers		
33 kV	0.0020	4
11 kV	0.0060	4
busbars		
33 kV	0.0010	2
11 kV	0.0010	2
lines		
33 kV	0.0460	8
11 kV	0.0650	5
line switches		
33 kV	0.01	3
11 kV	0.03	3

Table.4  
Parameters of TC-FLSFCL

Contents	Value	Number of Turns
<b>Winding 1, 2 and 3:</b>		
Self inductance of winding 1 ( $L_1$ )	42 mH	42 Turns
Self inductance of winding 2 ( $L_2$ )	1.63 mH	14 Turns
Self inductance of winding 3 ( $L_3$ )	0.9 mH, 1.63 mH, 3.8 mH, 42 mH	7 Turns, 14 Turns, 28 Turns, 42 Turns
<b>Solenoid magnet field winding:</b>		
Self inductance ( $L_f$ )	12 mH	
Winding resistance ( $R_f$ )	0.5 $\Omega$ (77 K)	

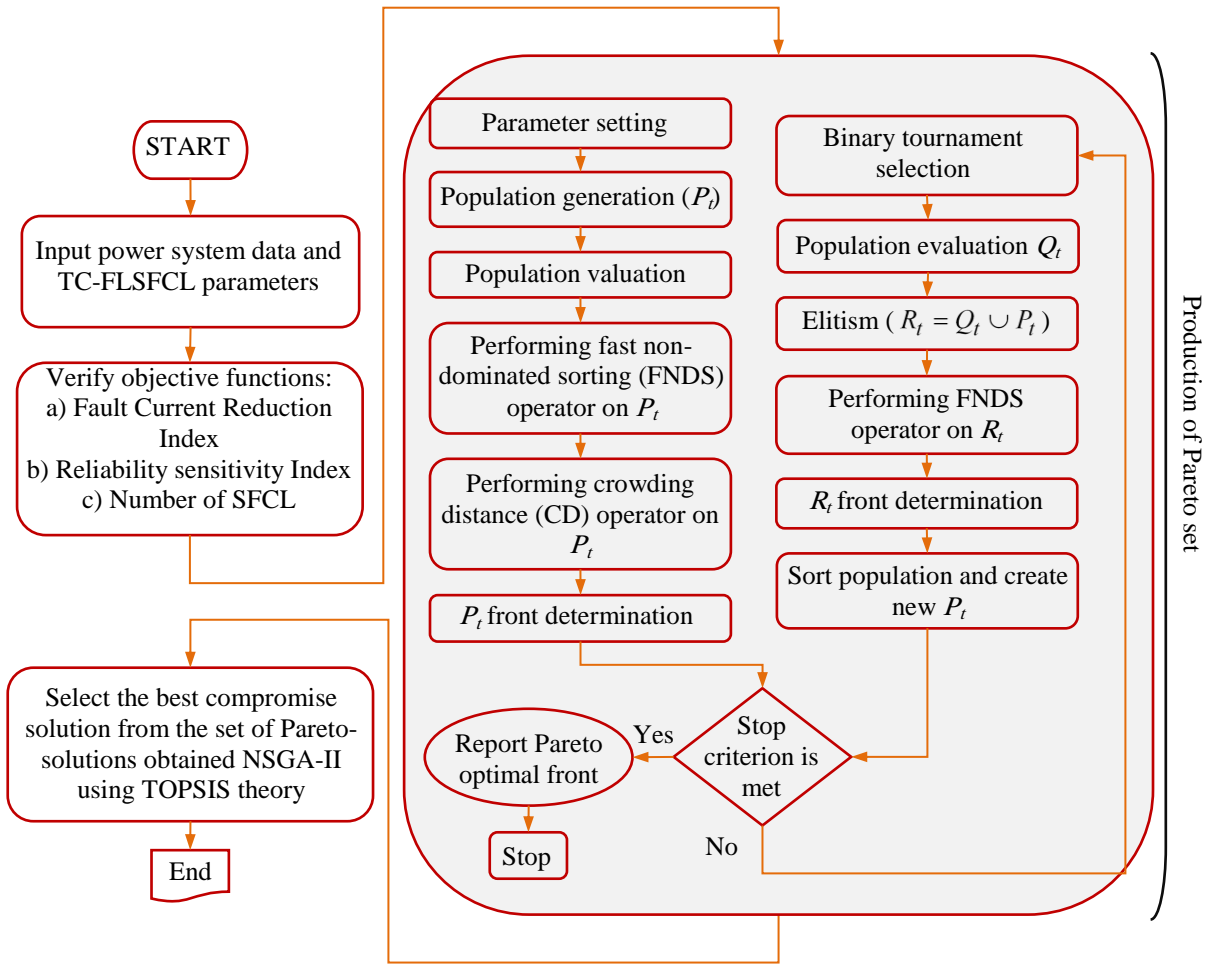


Fig. 5: Flowchart of the proposed method

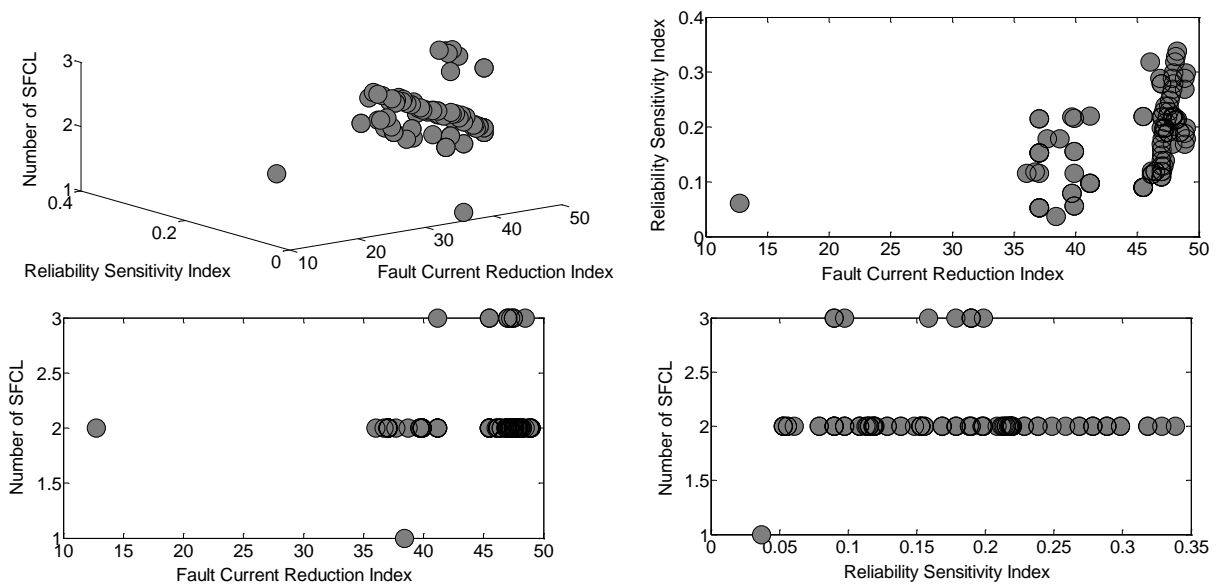


Fig.6. The Pareto-optimal set with NSGA-II in two-dimensional and three-dimensional objective space for TC-FLSFCL

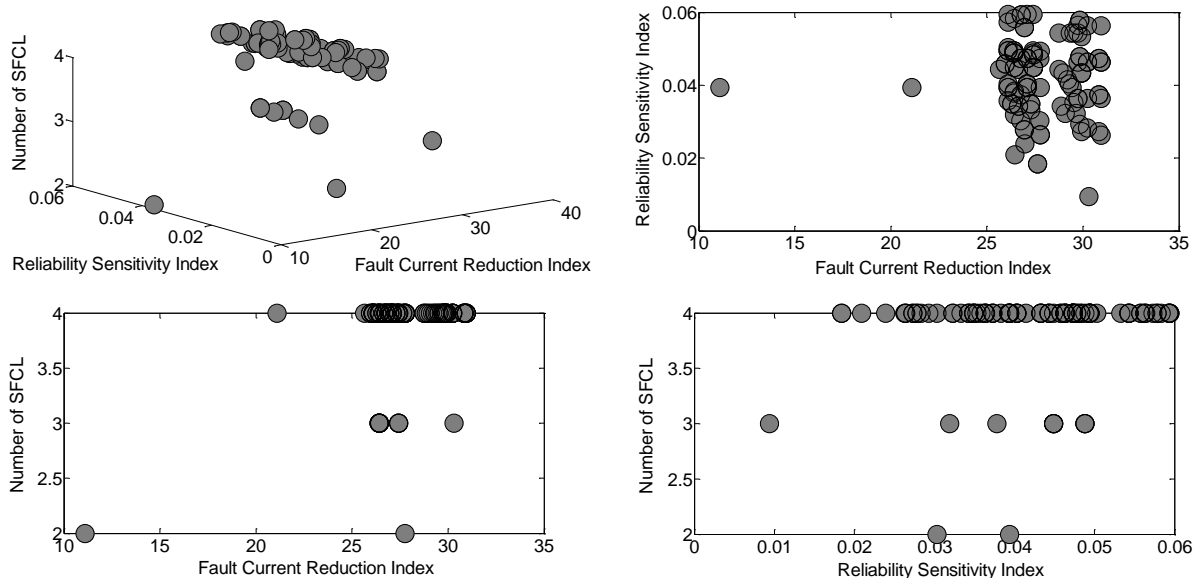


Fig.7. The Pareto-optimal set with NSGA-II in two-dimensional and three-dimensional objective space for RSFCL

Table.5  
SFCL placement and design results for two cases

SFCL NO	Case 1: RSFCL (Number of SFCL=4)				Case 2: TC-FLSFCL (Number of SFCL=2)			
	SFCL 1	SFCL 2	SFCL 3	SFCL 4	SFCL 1	SFCL 2	SFCL 1	SFCL 2
Parameters	Resistance of SFCL ( $\Omega$ )	Resistance of SFCL ( $\Omega$ )	Resistance of SFCL ( $\Omega$ )	Resistance of SFCL ( $\Omega$ )	$R_{NRHTSC}$ ( $\Omega$ )	Self inductance of winding 3	$R_{NRHTSC}$ ( $\Omega$ )	Self inductance of winding 3
Value	0.8147	0.9058	0.9134	0.6324	20.576	0.9 mH (7 Turns)	21.419	3.8 mH (28 Turns)
Location	Line 1	Line 60	Lin 21	Line 36	Line 19		Line 58	

Table.6  
Best compromise solution of NSGA-II and ordinary MOPSO with optimal placement and design using TOPSIS method

Objective functions	Case 1: RSFCL			Case 2: TC-FLSFCL		
	Number of SFCL	Fault current reduction index	Reliability sensitivity index	Number of SFCL	Fault current reduction index	Reliability sensitivity index
TOPSIS based NSGA-II	4	32.18	0.0592	2	48.357	0.1821
TOPSIS based MOPSO	4	31.915	0.0456	2	47.8491	0.1729

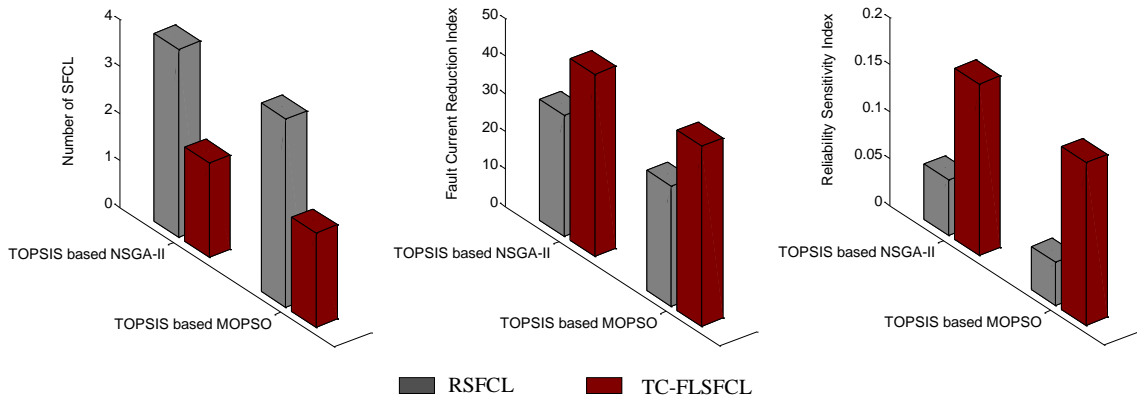


Fig.8. Comparison of the performances

## References

- [1] S. Kalsi, Applications of high temperature superconductors to electric power equipment, Wiley-IEEE Press, 2010.
- [2] E. Leung, B. Burley, N. Chitwood, H. Gurol, G. Miyata, D. Morris, *et al.*, "Design and development of a 15 kV, 20 kA HTS fault current limiter", IEEE Transactions on Applied Superconductivity, Vol.10, No.1, pp.832-835, 2000.
- [3] W. Paul, M. Chen, M. Lakner, J. Rhyner, D. Braun, and W. Lanz, "Fault current limiter based on high temperature superconductors—different concepts, test results, simulations, applications", Physica C: Superconductivity, Vol.354, No.1, pp.27-33, 2001.
- [4] S. Elschner, F. Breuer, M. Noe, T. Rettelbach, H. Walter, and J. Bock, "Manufacturing and testing of MCP 2212 bifilar coils for a 10 MVA fault current limiter", IEEE Transactions on Applied Superconductivity, Vol.13, No.2, pp.1980-1983, 2003.
- [5] H.-S. Choi, H.-M. Park, Y.-S. Cho, S.-H. Lim, and B.-S. Han, "Quench characteristics of current limiting elements in a flux-lock type superconducting fault current limiter", IEEE Transactions on Applied Superconductivity, Vol.16, No.2, pp.670-673, 2006.
- [6] S. H. Lim, H. S. Choi, and B. S. Han, "Operational characteristics of a flux-lock-type high-T<sub>c</sub> superconducting fault current limiter with a tap changer", IEEE Transactions on Applied Superconductivity, Vol.14, No.1, pp.82-86, 2004.
- [7] K. Hongesombut, Y. Mitani, and K. Tsuji, "Optimal location assignment and design of superconducting fault current limiters applied to loop power systems", IEEE Transactions on Applied Superconductivity, Vol.13, No.2, pp.1828-1831, 2003.
- [8] B. C. Sung, D. K. Park, J.-W. Park, and T. K. Ko, "Study on optimal location of a resistive SFCL applied to an electric power grid", IEEE Transactions on Applied Superconductivity, Vol.19, No.3, pp.2048-2052, 2009.
- [9] U. A. Khan, J. Seong, S. Lee, S. Lim, and B. Lee, "Feasibility Analysis of the Positioning of Superconducting Fault Current Limiters for the Smart Grid Application Using Simulink and SimPowerSystem", IEEE Transactions on Applied Superconductivity, Vol.21, No.3, pp.2165-2169, 2011.
- [10] J.-H. Teng and C.-N. Lu, "Optimum fault current limiter placement", in Intelligent Systems Applications to Power Systems, ISAP 2007, 2007, pp. 1-6.
- [11] J. Kumara, A. Atputharajah, J. Ekanayake, and F. Mumford, "Over current protection coordination of distribution networks with fault current limiters", in Power Engineering Society General Meeting, 2006.
- [12] W. El-Khattam and T. S. Sidhu, "Restoration of directional overcurrent relay coordination in distributed generation systems utilizing fault current limiter", IEEE Transactions on Power Delivery, Vol. 23, No. 2, pp. 576-585, 2008.
- [13] G. Didier, J. Leveque, and A. Rezzoug, "A novel approach to determine the optimal location of SFCL in electric power grid to improve power system stability", IEEE Transactions on Power Systems, Vol.28, No.99, pp.978-984, 2012.
- [14] M. Fotuhi-Firuzabad, F. Aminifar, and I. Rahmati, "Reliability study of HV substations equipped with the fault current limiter", IEEE Transactions on Power Delivery, Vol.27, No.2, pp.610-617, 2012.
- [15] S.-Y. Kim, W.-W. Kim, and J.-O. Kim, "Determining the location of superconducting fault current limiter considering distribution reliability", Generation, Transmission & Distribution, IET, Vol.6, No.3, pp.240-246, 2012.
- [16] K. Deb, Multi-objective optimization using evolutionary algorithms. Singapore: John Wiley and Sons, 2001.
- [17] K. Deb, A. Pratap, S. Agarwal, and T. Meyarivan, "A fast and elitist multiobjective genetic algorithm: NSGA-II", Evolutionary Computation, IEEE Transactions on, Vol.6, No.2, pp.182-197, 2002.
- [18] P. Schubert and W. Dettling, "Extended Web Assessment Method (EWAM)-evaluation of e-commerce applications from the customer's viewpoint", in System Sciences, 2002. HICSS. Proceedings of the 35th Annual Hawaii International Conference on, 2002.
- [19] J. Wu, J. Sun, Y. Zha, and L. Liang, "Ranking approach of cross-efficiency based on improved TOPSIS technique", Journal of Systems Engineering and Electronics, Vol.22, No.4, pp.604-608, 2011.
- [20] R. Billinton, R. N. Allan, and R. N. Allan, Reliability evaluation of power systems vol. 2: Plenum Press New York, 1984.
- [21] R. N. Allan, R. Billinton, I. Sjarief, L. Goel, and K. So, "A reliability test system for educational purposes-basic distribution system data and results", IEEE Transactions on Power Systems, Vol.6, No.2, pp.813-820, 1991.
- [22] A. Chowdhury and D. O. Koval, "Application of customer interruption costs in transmission network reliability planning", IEEE Transactions on Industry Applications, Vol.37, No.6, pp.1590-1596, 2001.